GEODYNAMICAL IMPACT OF RIVER MEANDERING ON RIPARIAN PLANT COMMUNITIES

Dr. N.L. Dongre, IPS, Ph.D., DLitt**

Before the Yarlung Zangbo leaves China to flow into the Arunachal Pradesh region of India and become the Brahmaputra, it makes a dramatic turn to the south, known as the Great Bend. The fundamental role of Brahmaputra River morpho-dynamics and hydrology for the establishment and evolution of riparian vegetation. The effects of the river band induced processes on the plant communities along a riparian transect. The shape of each function depends on the prevailing meandering mechanism

[1] The study generates the dynamics of meandering rivers impact on the formation of riparian vegetation patterns. To this aim, a model coupling river dynamics and riparian vegetation evolution was developed. Meandering dynamics were simulated with a fluid dynamical model using shallow water equations on an erodible bed. The model of riparian vegetation takes into account many actions caused by the river, i.e., water table oscillations, floods, and sedimentation. A logistic law and an exponential decay were used to model the increase and decrease in the biomass, respectively, consequent to river meandering and migration. The numerical simulation by the model emphasizes the river dynamics can induce typical vegetation patterns that are identical to real riparian landscapes. With solid examples quoted from important rivers, it is investigated the facts regarding impact of river meandering on riparian vegetation. Despite the fact that traditional geological approach considers vegetation as a static element to study of river meandering dynamics should be coupled with the riparian vegetation evolution. To this end the model of meandering river is coupled with a process based model for the riparian bio-mas dynamics. The result highlights (1) the remarkable and relevant river-vegetation interacts to meandering evolution and (2) the role of temporal scales of vegetation growth and decay in interaction to the typical dynamic scales evolution and river migration.

Keywords: River Meandering, Riparian, biotic ecosystem river bank, Kinoshita curve

---

**Dr. N.L. Dongre
C-14 Jaypee Nagar Rewa 486450
Email: - nl.dongre@jalindia.co.in dongrenl@gmail.com
Mobile No. 7869918077, 09425152076

1. Introduction

[2] The interaction between a meandering river and its surrounding riparian vegetation has attracted much interest in recent years because of their remarkable environmental management implications. Riparian vegetation is one of the biotic communities living near to the river banks, which is sustained by and interacts with the stream to a great extent. Several definitions of the riparian zone can be found in literature. The riparian ecosystem is a very complex zone that usually occurs as an ecotone between aquatic and upland ecosystems, but with distinct vegetation and soil characteristics (*Malanson* [1993]. The riparian zone is an area which encompasses the stream channel between the low and high water marks where vegetation may be influenced by elevated water tables or flooding and the ability of the soils to hold water (*Naiman and Decamps,* 1997). More recently, *Mitsch and Gosselink* [2000] defined the riparian zone as the land adjacent to water that is, at least periodically, influenced by flooding.

[3] The riparian vegetation along meandering rivers investigates whether morphological river dynamics are able to significantly affect the formation of spatial vegetation patterns. It is a fact that the morphodynamics and hydrology of meandering rivers affect several riparian processes to a great extent Instances are that spatial patterns of plant succession along river transects depend on river migration, which erodes the concave bank and deposits sediments on the opposite point bar. Interactions among river movements, sedimentation processes, and vegetation cause the formation of arcuate tree bands parallel to the river axis. Fluvial migration also controls the texture of riparian soils, influencing the soil moisture balance and thereby affecting the establishment of riparian plants. Oxbow lakes, due to meander cutoffs, also contribute to the mosaicism of riparian landscapes. River hydrology, i.e., the variation of river flow, induces oscillations in water levels in the stream and in the groundwater table, thus influencing the transport of water, sediments, seeds, and nutrients. Floods and discharge recessions affect the survival of seedlings after germination. Floods can also disturb riparian vegetation, by causing uprooting, anoxia or burial. As riparian floodplains of meandering rivers usually have a ridge and swale topography, vegetation patches differ, depending on the adaptation of the species to the hydroperiod.

[4] The cause of these activities by the river is that vegetation can have "a predictable development based on the distance from the river" such as the river can induce riparian vegetation patterns. Figure 1a ,the Wainganga river shows an example: Sediment deposition is visible close to the internal bank of the meanders, where the density of vegetation increases moving away from the river. Some examples of river-induced patterns are the regular zonation of the communities in the Yamuna and the Tawa of India, where forests along meandering rivers usually take the form of arcuate, parallel bands of even aged trees. (Figure 1 b and 1c).

[5] Several other factors, such as climate conditions, the presence of animals, harvesting, fire, grazing, diseases, large wood debris, and human actions, are able to influence the formation of riparian vegetation patterns, and the patterns observable in nature are often the result of the concurrent action of many processes, both fluvial and river independent. The attention is focused on the morphological river evolution in order to isolate its contribution to pattern formation and to the type of patterns that are likely to emerge. Owing to the complexity of the problem, the role of meander evolution before cutoff occurrence has been investigated, without considering the formation of oxbow lakes.

[6] Many conceptual-qualitative models regarding riparian vegetation evolution were proposed in the past; however, to our knowledge, only a few quantitative models have been formulated due to the influence of floods and water table fluctuations on vegetation growth. More recently, in the context of ecosystem restoration, *Mahoney and Rood* [1998] proposed a predictive model for poplars in western Canadian rivers, and *Richter and Richter* [2000] developed a model that is able to show the importance of flooding on riparian vegetation along meandering rivers. These models are important steps in the process of understanding the interactions between river and riparian vegetation, but they do not focus on morphological dynamics.

Figure: 1.a, Riparian landscape along the Wainganga River (Balaghat). A bare soil zone is evident at the convex bank of the meander and the biomass increases, moving away from the river as a dense wood is reached. This vegetation pattern seems to be generated by river migration, which deposits forest sediments on the internal bank, where the vegetation starts growing, thus giving rise to low biomass zone close to the bank

Figure: 1. b. Yamuna River and farmlands outskirts of Delhi, results of the river induced processes is the formation of spatial patterns of riparian vegetation, which depends to a great extent on their distance from the river

Figure: 1.c, Tawa River. This picture is an evident consequence of the meandering dynamics, which are able to generate patterns of riparian plant community. The active role of meandering is responsible for the different planforms obtained using different transversal vegetation distribution. The meandering dynamics generates a pattern where high density vegetation zone are pre-dominant close to the meander apexes

The approach is that it couples a fluid dynamic model, providing a realistic process based simulation of river evolution, with a model of riparian vegetation along a river transect. In particular, it is modeled the growth and enlargement of the meanders and the consequent response of vegetation to river migration. The former aspect was carried out by simulating shallow water equations on an erodible bed. The riparian vegetation dynamics are modeled taking into account (1) some of the key effects of hydrological and geomorphological processes on riparian vegetation (water table oscillations, flooding, and sedimentation, and (2) the increase or decrease in vegetation biomass, which depends on the distance of the vegetation sites from the river bank. As a river migrates, the riparian system continuously evolves through transitory states where characteristic patterns emerge, provided the typical time-scales of the vegetation and the river evolution are comparable. In this model, it is considered only the one-way influence of the river on riparian vegetation, while the feedback of vegetation on river morphology has been neglected.

[7] The approach followed in the modeling was to retain some key processes, both in river morphodynamics and vegetation dynamics, while keeping the model as simple as possible. In this way, it is believed that the obtained results describe the fundamental morphodynamic-induced components that exist in several real riparian patterns, as some qualitative comparisons with real data seem to confirm. To this end, and in accordance with recent results by *Van De Wiel and Darby* [2004], it is referred to vegetation biomass without taking the diversity of species into account.

2. Methods

2.1. Riparian Vegetation Model

[8] The river plays a basic role to establishment the growth of riparian vegetation since it provides water, nutrients, and sediments through flooding and the ground-water flow. As recollected in section 1, such an influence occurs by means of many physical and biological processes. In this work, it is summarized the effects of the main river-induced processes on riparian vegetation using three typical

distributions of biomass densities along a river transect. Such distributions depend on the dominant hydro-logical mechanisms that affect riparian vegetation.

[9] To define the modeling plan it is assumed that the river does not migrate across the floodplain. Let us define D as the distance of a generic vegetation plot from the river bank, $V_{st}(D)$ as the corresponding density of the vegetation biomass (the subscript stands for the steady conditions of the river morphology), and $V_{st,max}$ as its maximum value. Finally, L is the distance that encompasses the significant variations in biomass density; this distance can be assumed as the typical length scale of the transversal variations of the biomass density.

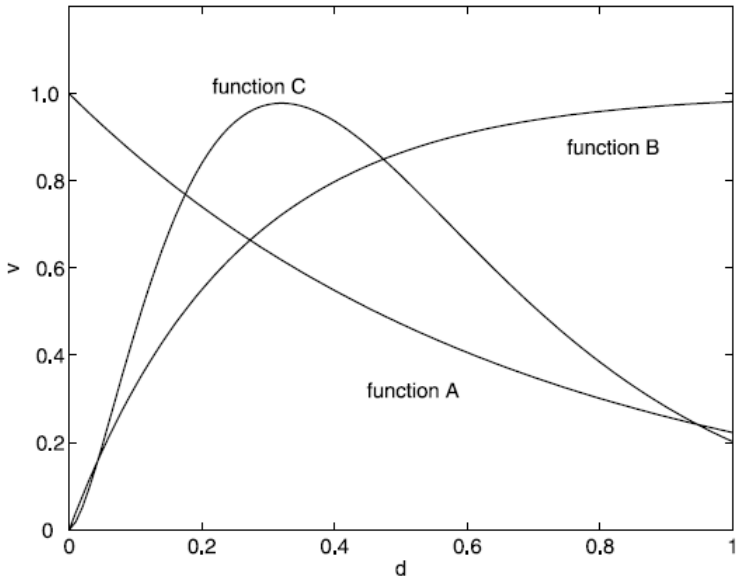

Figure 2. Example of density functions A, B and C ($\alpha = 30, \beta_1 = 1.5, \beta_2 = 4, \beta_3 = 5, \eta = 1.6$).

[10] The typical shape of density distribution emerges when the control of the water table depth is the main action of a river on the riparian vegetation ecosystem. In these cases, riparian vegetation can draw water and nutrients mainly in the proximity of a river, while, moving away from the river bank, vegetation thins out, because of the increased depth of the water table. This situation is typical of semi-arid regions, where the main water supply comes from the river *[Carr,* 1998]. However, similar patterns have also been documented in mild or humid climate zones. It is noticed that along the Wainganga river , the proximal riparian vegetation closer to the channel is denser than the distal forest'. A possible mathematical expression (hereinafter indicated as function A) of biomass density as a function of the distance is

$$v_{st}(d) = e^{-\beta_1 d}, \tag{1}$$

where $v_{st} = V_{st}/V_{st,max}$, $d = D/L$, and β_1 is a curve parameter. In such a way, the biomass density has a maximum at the river bank (i.e, at $D = d = 0$) and then decreases (see Figure 2).

[11] The destructive action by floods is the main factor affecting riparian vegetation, another category of density functions can be suggested. In this case, the vegetation close to the river is destroyed by extirpation or dies from burial under the transported sediments and from anoxia because of the prolonged persistence of high water levels *[Bradley and Smith,* 1986]. The typical length, *L,* is linked to the distance from the river banks that floods can reach. In this case, the density of the biomass considered in the model is (function B)

$$v_{st}(d) = 1 - e^{-\beta_2 d}, \tag{2}$$

where β_2 is a parameter. The biomass density is therefore smaller close to the river bank and increases moving away from the river (see Figure 2)

[12] It is considered that the concurrent action of the water table, sedimentation and flooding. In this situation, the riparian vegetation close to the river banks is mainly influenced by flood disturbances, while vegetation far from the river suffers from a declining water table and interspecific competition. Therefore it is likely that the riparian vegetation density reaches a maximum at a certain distance from the river. A density function shaped in this way was documented by *Nanson and Beach* [1977]. The authors analyzed tree density and succession in the Tawa and Denwa river (India) and found a linear relationship between river distance and plant age. The total tree density for both ridges and swales achieves maximum values on surfaces that are approximately 100 years in age, and rapidly declines to low values. In this case, the normalized density function (function C) can be modeled as

$$v_{st}(d) = ad^{\eta}e^{-\beta_3 d}, \tag{3}$$

where a, η and β_3 are curve parameters.

[13] The influence of river migration on riparian vegetation is analyzed. When the river moves, the distance of the vegetation sites from the river changes and riparian vegetation tends to the stationary value of density that corresponds to the actual distance from the river bank. This temporal evolution of biomass density is described by a curve of a logistic type, if the biomass increases (the river becomes closer in the case of function A), or by an exponential decay, if the biomass density decreases.

[14] The logistic curve is a well-known, simple and commonly accepted model of population growth *[Tsoularis and Wallace,* 2002; *Thornley and France,* 2005]. Accordingly, it is modeled that the increase in the normalized density biomass, *v(d, t),* in a site at a dimensionless distance, *d,* from the river bank as
scale of the vegetation was not dependent on the distance from the river bank.

$$\frac{\partial v(d,t)}{\partial t} = r \cdot v(d,t) \cdot \left(1 - \frac{v(d,t)}{v_{st}(d)}\right), \tag{4}$$

where t is the dimensionless time (section 3), r is the growth rate and $v_{st}(d)$represents the so-called carrying capacity. In this model, the latter is the maximum sustainable biomass density corresponding to the distance, *d,* from the river bank. An important parameter of the logistic curve is the growth rate, which determines the temporal scale of vegetation growth, $T_{vg.}$ It is defined $T_{vg.}$as the time necessary to reach a fixed value, $\epsilon_2 V_{\mathrm{st,max}}$ (with $\epsilon_2 \simeq 1$), starting from$\epsilon_2 V_{\mathrm{st,max}}$ ($\epsilon_1 \ll 1$), namely

$$T_{vg} = \mathrm{In}\left(\frac{\epsilon_1 - 1}{\epsilon_1}\frac{\epsilon_2}{\epsilon_2 - 1}\right)^{1/r} \tag{5}$$

For example, if $\epsilon_1 = 0.05$, $\epsilon_2 = 0.95$, and $r = 0.1$, it is obtained $T_{vg} \simeq$ 50 years. The mathematical form (4) was chosen so that the temporal scale of the vegetation was not dependent on the distance from the river bank.

[15] On the contrary, if, owing to river migration, the biomass of the riparian vegetation plots needs to decrease to a new, lower assigned value, an exponential decay is used in the model, that is,

$$\frac{\partial v(d,t)}{\partial t} = -\gamma\big(v(d,t) - v_{st}(d)\big), \tag{6}$$

where γ is the decay constant. In this case a temporal scale of vegetation decay, $T_{vd,}$can be defined as the time necessary to reach $\epsilon_1 V_{st,\mathrm{max}}$ from $\epsilon_2 V_{st,\mathrm{max}}$,

$$T_{wd} = \mathrm{In}\left(\frac{\epsilon_2}{\epsilon_1}\right)^{1/\gamma} \tag{7}$$

For example, if γ= 0.1, ϵ_1 = 0.05, and ϵ_2 = 0.95, it is obtained $T_{vd} \simeq 30$ years. In the following, only T_v is written when $T_{vg} \simeq T_{vd}$

2.2. River Meandering Model

[16] The core mechanism of river meandering is the action of a helicoidal curvature-driven secondary flow which activates an inward lateral sediment flux on the bed. The consequent transversal shoaling of the bed topography, with the formation of point bars, triggers a topography-driven secondary flow and a topographic steering of the longitudinal flow *[Dietrich and Smith,* 1983], which, in turn, induces outward bank erosion. The transport of momentum induces a stream-wise phase lag between the curvature and the flow field establishing a spatial memory in the downstream propagation influence *[Howard,* 1984] and, consequently, in both the downstream skewness of the shape of the meander loops, and in the downstream migration *[Parker et al.,* 1983]. Curvature therefore increases and the process is self-sustained.

[17] The morphological evolution is characterized by a continuous growth in amplitude of meanders and increase in river sinuosity till, to prevent self-intersection, cutoff takes place and short reaches of the river, named oxbow lakes, are abandoned. The resultant morphological dynamics are known to be driven by both linear and nonlinear processes while the interaction between cutoff events and bend elongations moves the system toward a statistical steady state.

[18] In order to realistically simulate meandering dynamics, the fluid dynamical model by *Ikeda et al.* [1981] was adopted. Despite its simplicity, this model is based on a consistent, process-based analysis of the physical processes, through the St.Venant equations for a shallow steady turbulent flow in a sinuous channel, and it allows some basic characteristics of real meanders to be reproduced, namely wavelength selection, elongation, deformation and downstream migration. For these reasons, the model by *Ikeda et al.* [1981] has been used in several numerical investigation *[Beck,* 1984; *Sun et al.,* 1996] and it represents a good compromise between the process-based description of the fluid dynamics and an acceptable numerical complexity for the purposes of the present work.

[19] The local rate of river migration, $\zeta(s)$, is assumed to be proportional to the local excess-bank longitudinal velocity $u_b(s) = u(s,b) - U$,where *s* is the longitudinal coordinate, $u(s,b)$ is the value of the depth-averaged longitudinal velocity close to the bank, b is the channel half width, and *U* is the mean velocity *[Ikeda and Parker,* 1989]. It follows that $\zeta = E.u_b$,where *E* is the erodibility coefficient that depends on the geotechnical characteristics of the bank. This hypothesis was confirmed by field investigations *[Pizzuto and Meckelnburg,* 1989] and is commonly used in numerical simulations *[Howard,* 1984; *Stlum,* 1996]. In this study, a constant value of *E* is used, without taking into account the possible dependence of the erodibility coefficient on the biomass density.

[20] In the *Ikeda et al.* [1981] model, the computation of u_b is provided through the linear perturbation of the depth averaged equation for the longitudinal and transversal momentum and mass conservation written in curvilinear coordinates. The effects of secondary currents on bedload transport are modeled through of the semi-theoretical linear relationship

$$\frac{\partial \eta}{\partial n} = -AC, \tag{8}$$

where η is the bed topography elevation, *n* is the transversal coordinate (normal to the river axis), *C* is the curvature of the river axis, and *A* is the lateral slope factor which depends on the friction factor, C_f, the turbulence closure model, and the Shield stress. The previous relationship implicitly assumes a triangular bed topography and neglects the coupled dynamics between the bed sediment transport and water flow. However, the effect of these simplifications can be minimized if the slope factor *A* is not considered as a constant value (as in the original *Ikeda et al.* [1981] model) but is calculated on the basis of a separated advanced solution of the secondary currents. Accordingly, the procedure by *Johannesson and Parker* [1989] was followed using their equation (34c) at each computational step.

[21] Finally, the solution of the *Ikeda et al.* [1981] model reads

$$u_b = -bUC + \frac{UbC_f}{H}[F^2 + A + 1]\int_0^s e^{-\frac{2C_f}{H}(s-z)}C(Z)dz, \qquad (9)$$

where H is the average depth and F is the Froude number. Once the local excess-bank velocity, u_b, is evaluated along the river, it is possible to obtain the local rate of bank erosion and to let the river migrate accordingly. The evolution of the river morphology can be simulated by iterating this algorithm. Figure 3 shows an example of the evolution assuming the Kinoshita curve ($\theta_0 = 30°$) as the initial condition *[Kinoshita,* 1961]. The Kinoshita curve describes the meander geometry in a simple way according to

$$\theta = \theta_0 \sin ks + \theta_1 \sin 3ks + \theta_2 \cos 3ks \qquad (10)$$

where s is a curvilinear abscissa, θ is the angle between the tangent to the curve and a reference axis, θ_0 is the maximum direction angle, while the relationships for the 'skewing' coefficient θ_1, the 'fattening' coefficient θ_2 and the dominant wave number k read *{Parker et al.,* 1983]

$$\theta_1 = \frac{\theta_0^3}{192}, \theta_2 = \theta_0^3\frac{\sqrt{P}}{128}, k = k_c\left[1 - \frac{\theta_0^2}{12}\frac{(2A+5F^2)}{P}\right], \qquad (11)$$

with $P = 2(A + F^2)$ and $k_c = \sqrt{PC_f}$ Finally, T_r, the time that the river spends to move a length equal to its mean half wavelength $\lambda/2$ starting from a Kinoshita-shaped initial condition with$\theta = \theta_0$, is assumed as a typical temporal scale of the river evolution.

3. Results and Discussion

[22] The typical vegetation patterns that can be obtained through simulations are described in this section. The Kinoshita river morphology with $\theta_0 = 30°$ was assumed as the initial condition of the river. This is a slightly sinuous configuration that well represents a typical real meander in its initial expansion phase *[Carson and Lapointe,* 1983; *Parker et al.,* 1983]. Starting from this condition, the fluvial evolution was simulated using the *Ikeda et al.* [1981] model until the cutoff event occurred. As local fluvial dynamics are mainly influenced by the upstream morphology *[Johannesson and Parker,* 1989], a regular series of meanders was simulated to correctly reproduce the evolution of the central meander. These boundary conditions give rise to a strong periodicity of vegetation patterns (visible in the following figures) that, however, does not invalidate the realistic vegetation behavior around the single meander. The values of the hydraulic parameters used in the simulations (C_f= 0.0032 and F = 0.4) are typical of several river systems around the world *[Parker and Johannesson,* 1989].

[23] With regard to the riparian vegetation density, the stationary condition, V_{st}, was assumed as the initial condition. As the migration velocity is proportional to the meander curvature (see equation (9)), the fluvial evolution is in fact very slow for $\theta < \theta_0$. Two cases were explored: (1) when the temporal scale of the vegetation is much lower than that of the river $(T_{vg} \ll T_r, T_{vg} \ll T_r)$ and (2) when the temporal scale of the vegetation, T_v and that of the river, T_r are comparable $(T_{vg} \ll T_r, T_{vg} \ll T_r)$. In particular, the following ranges were investigated: $T_{vg} = T_{vd} = (0.005 \div 10)T_r$ and $T_{vg} = (0.05 \div 20)T_{vd}$. The case with was excluded as it does not seem realistic that the temporal scale of vegetation could be much greater than that of the river, which is usually of the order of 10^1-10^2 years [e.g., *Hughes,* 1997].

[24] As far as the spatial scales are concerned, as the river is only able to induce vegetation patterns if its morphological spatial scale (equal to the mean half wavelength$\lambda/2$) is comparable with the vegetation one, L, weset $\lambda/2 \simeq L$.

[25] The floodplain was divided into square cells of approximately $10^{-2}L$, this being an adequate spatial resolution compared with the river width($b \simeq 10^{-2}L$.). The vegetation biomass was considered uniform in each cell, and its dynamics were modeled according to equations (4) and (6). The time steps for the river morphology and vegetation updates were chosen approximately equal to $10^{-4}T_r$, and

$10^{-3}T_r$, respectively (for other numerical details concerning the river morphology simulation, reference can be made to *Sun et al.* [1996] and *Camporeale et al.* [2005]).

[26] The river axis is represented in white in Figures 4-7 (the flow is from right to left) and the vegetation in shades of green: the darker the green, the greater the biomass. Reference was made to the dimensionless time $t = T/T_I$, where T is the simulation time in years.

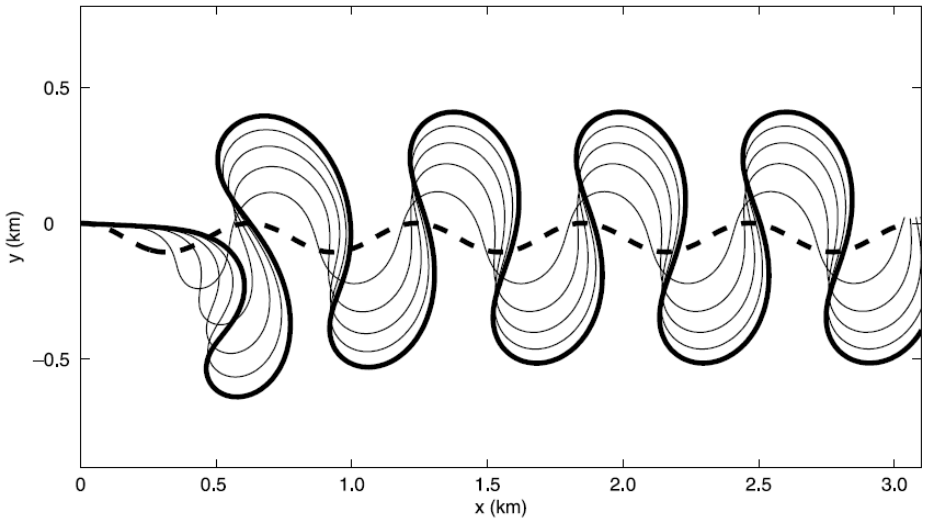

Figure 3. Example of a 200-year river evolution starting from a river morphology shaped like the Kinoshita curve (θ_0= 30°, $E = 3 \cdot 10^{-7}$). The dashed curve is the river axis at t = 0. The thick curve is the final morphology. The other lines represent Intermediate river configurations plotted every 40 years.

3.1. Vegetation Temporal Scale Much Lower Than the River Scale ($T_v \ll T_r$)

[27] When the temporal scale of the vegetation, T_v, is much lower than that of river morphodynamics, T_r, the riparian vegetation 'follows' the morphological evolution of the river, that is, the vegetation continuously takes on the density values relative morphologies drawn by the river during its migration. An example is shown in Figures 4a-4c, which was obtained using density function C (similar type of vegetation patterns also occur for $T_v \simeq T_r$ till $\theta < \theta_0$) Similar results were also obtained for functions A and B. Function A follows the river movement for temporal scales of vegetation lower than those necessary for functions B or C. This is due to the position of the maximum value of density, which is close to the river bank for function A.

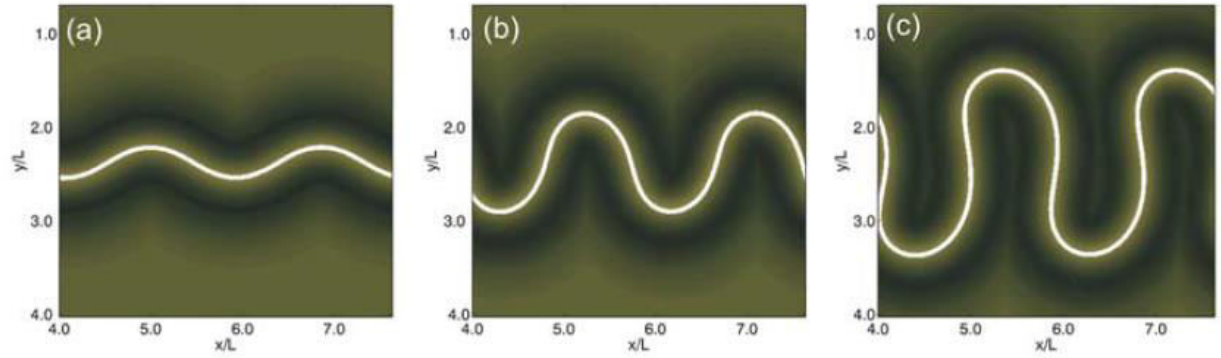

Figure 4. The $T_v \ll T_r$ case. Simulations with density function C at (a) t = 0, (b) t = 0.1, and (c) t = 0.3.

3.2. Vegetation Temporal Scale Comparable to the River Scale $(T_{vg} \simeq T_r, T_{vd} \simeq T_r)$

[28] When the temporal scale of vegetation dynamics, T_v, and that of river morphodynamics, T_r, are comparable, i.e., when the time the vegetation takes to grow from a very low density value to the maximum density is of the same order of magnitude as the time necessary for the river to move the typical length L, interesting vegetation patterns are obtained.

[29] The case when $T_{vg} = T_{vd}$ is first considered. If function A is used, the typical pattern shown in Figure 5a is obtained. A band of low biomass close to the internal part of the meander, oriented toward the river migration direction can be noted, while the external sites have higher biomass values. A quite sharp boundary separates the low biomass zone from the one with high biomass which is found between the meander inflections. Moreover, the vegetation biomass assumes lower values than those in stationary conditions at the cut bank. Also in the case of function B, where the maximum density $V_{st,\max}$ is at distance $d = 1$ from the river, it can be observed that the fluvial migration produces vegetation patterns that are similar to the previous one (see Figure 5b). However, it should be noted that, because of the different positions of the maximum of function B and function A, the aforementioned boundary between high and low biomass zones is less marked than in the previous case (Figure 5a). Finally, an example of patterns that originated using function C is shown in Figure 5c. The peculiar aspect of these patterns is a high density biomass strip, surrounded by lower densities, between the two inflection points of the meander.

[30] To validate the results, it is analyzed many aerial and remote-sensing images showing vegetation patterns along meandering rivers around the world. Most patters show the same main features it is obtained from the model and which are stressed in several papers, such as the zone of low biomass density in the internal part of the meander due to the migration of the channel Figures 6a, plot 1, through 6c, plot 2, report some comparisons with examples of real vegetation patterns. The pattern simulated using function A (Figure 6a, plot 1) closely resembles the riparian vegetation developed along the banks of the Denwa River (India) (Figure 6a, plot 2). Figure 6b, plot 1, instead refers to a vegetation pattern obtained with function B. It is compared with the riparian vegetation of the Wainganga river (India) (Figure 6b, plot 2), where the observations regarding the importance of flooding in the riparian ecosystem justify the adoption of function B. Both in the real landscape and in the simulated one, the resemblance in the vegetation classes reflects the river movement: The bare soil zones are close to the convex fluvial banks and moving away from the river, the vegetation biomass increases as long as values characteristic of nonflooded forests are reached.

[31] An example of a pattern obtained with function C (shown in Figure 6c, plot 1) is compared with the riparian vegetation that surrounds a portion of the Brahmaputra river shown in Figure 6c, plot 2 . The comparison also looks positive in this subject: In both figures, if the images are observed starting from the internal bank of the meander and going toward the floodplain, a large zone with a low vegetation density is clearly visible, and this is followed by another one where the biomass is thicker.

[32] The subjects in which only one of the two vegetation scales (T_{vg} or T_{vd}) is comparable with T_r, while the other becomes lower than the river timescale T_r were also investigated. The typical pattern that derives from function A when $T_{vg} > T_{vd}$ is shown in Figure 7a. This is very similar to the one shown in Figure 5a: The zone with low vegetation density is much extended inside the meander, while the biomass increases close to the inflection points, which move slower than the remaining part of the meander.

[33] An example of a vegetation pattern obtained with function B for $T_{vg} < T_{vd}$ is plotted in Figure 7b. This pattern is qualitatively different from the previous ones. In this case, the vegetation in the internal part of the meander partially follows the river movement, and, as a consequence, there is no wide low density zone. The reason for this is that, as the vegetation growth is faster than its decrease, the sites where the distance from the river increases (i.e. those at the internal bank) reach stationary density values in a short time. Those areas where the river approaches, instead, do not decrease in density with the same velocity. The density values at the cut bank are therefore higher than those one would expect in steady conditions

[34] The pattern obtained with function C for $T_{vg} > T_{vd}$ is shown in Figures 7c-7d. The relevant aspect of this pattern is that, in the first stages of meander formation, two distinct high biomass zones

form in the internal part of the meander (see Figure 7c). These zones tend to unify during the morphological evolution of the meander thereby forming a continuous zone between the inflection points of the river (Figure 7d).

4. Summary and Conclusions

[35] A model dynamically coupling some key features of riparian vegetation with river meandering evolution has been developed to investigate the influence of fluvial

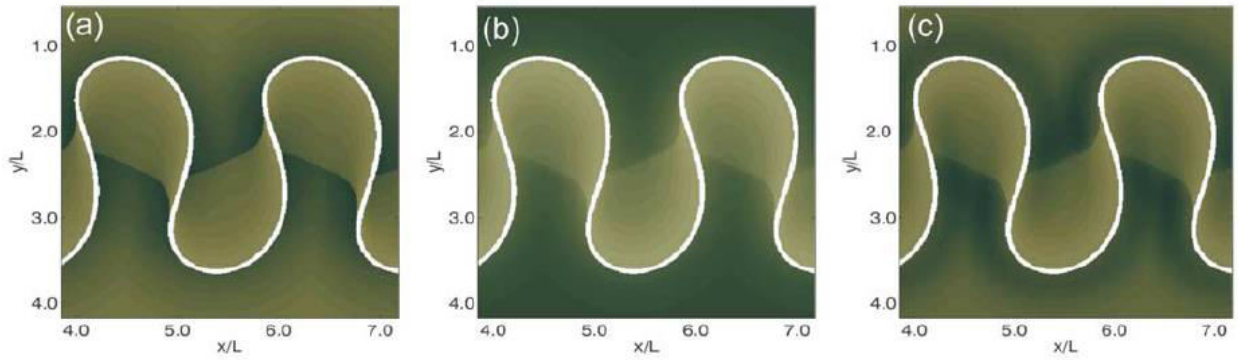

Figure 5. The $T_v \simeq T_r$ case$(t \simeq 0.5)$. (a) Pattern simulated with function A. (b) Simulation with function B. (c) Pattern corresponding to function C.

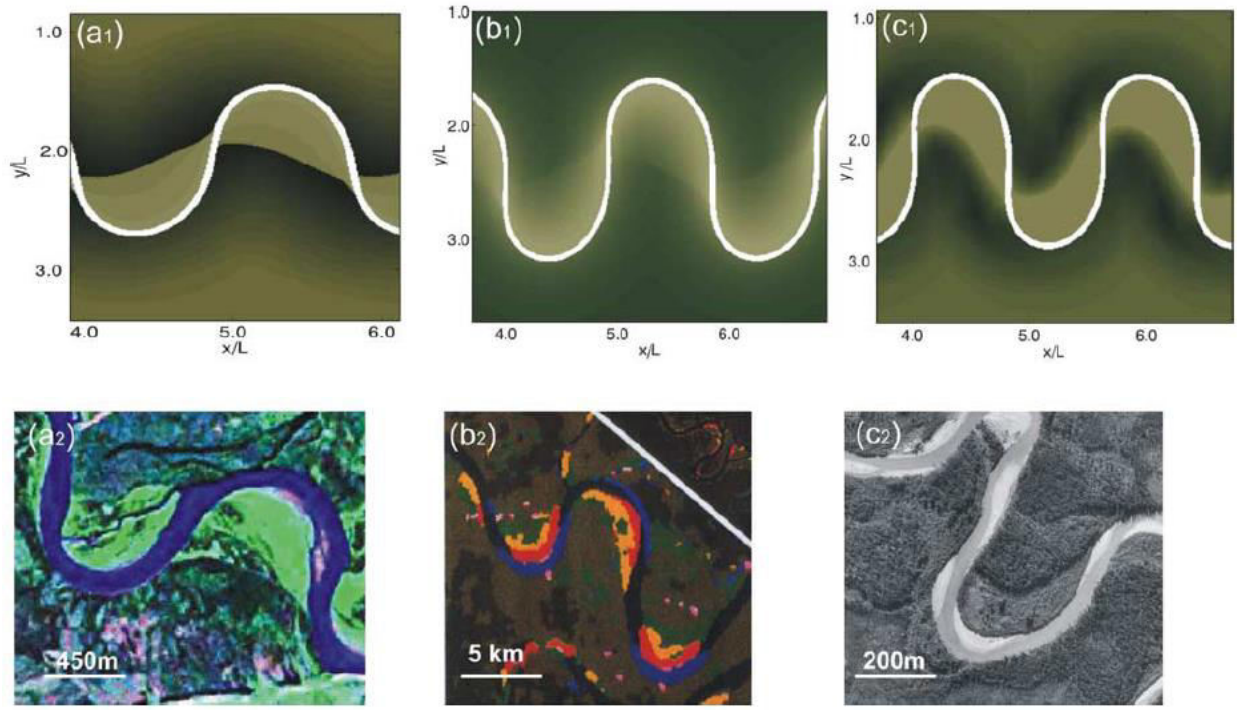

Figure 6. The $T_v \simeq T_r$ case. (a) Plot 1, pattern simulated with function A at t = 0.15(T_v = T_r = 1.0); plot 2, real landscape of the Denwa river (India). The picture is a composite image (ETM+ 7-4-2 bands) where the bare soil appears pink or magenta, the vegetation in shades of green and the river in blue or black. (b) Plot 1, simulation carried on with function B at $t \simeq 0.2$; plot 2, classification of the riparian vegetation of the Wainganga river. The red class represents deposition sites, the yellow class represents established primary succession sites, the bright green represents young forest with swamp vegetation in swales and, the light green represents stable floodplain vegetation, while the dark green is nonflooded forest. (c) Plot 1, simulation with density function C at $t \simeq 0.2$; plot 2, real landscape along the Narbada river.

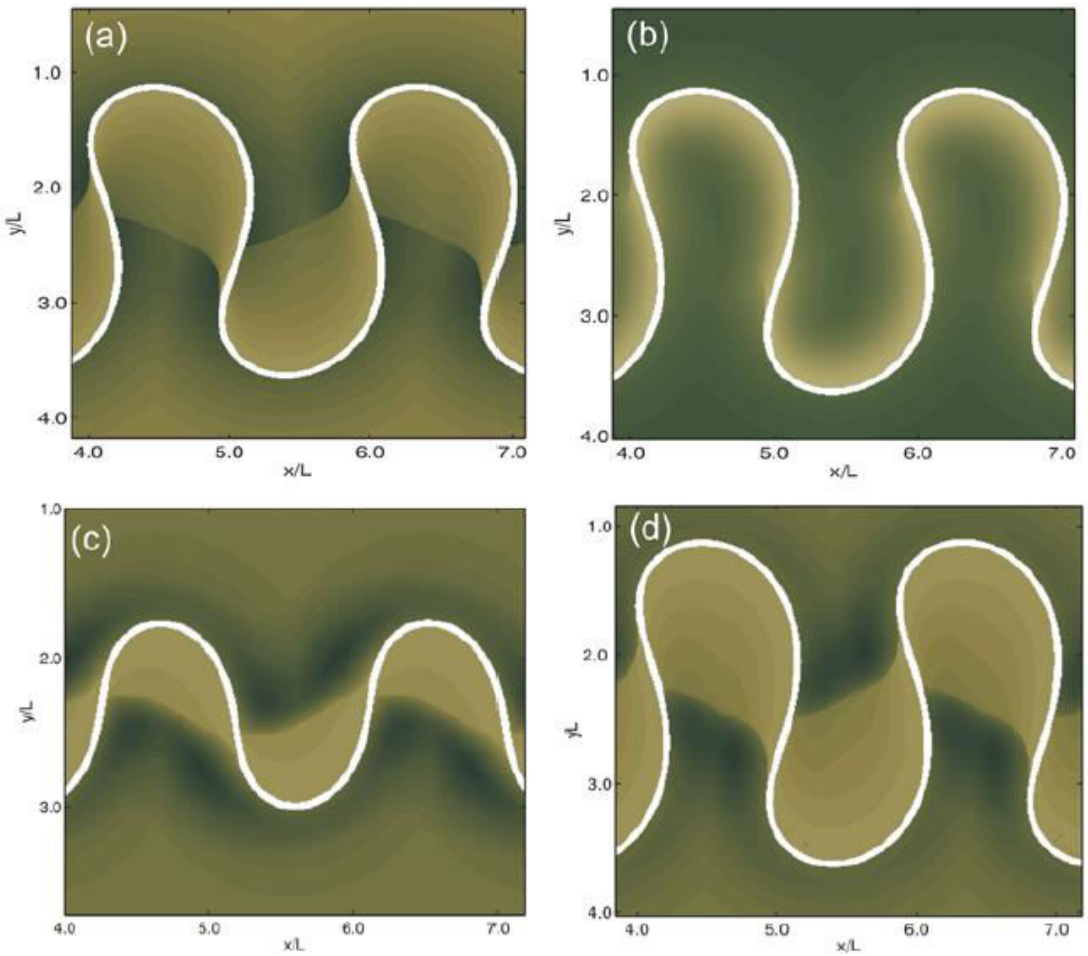

Figure 7. The $T_{vg} \neq T_{vd}$ case. (a) Pattern simulated with function A and $T_{vg} > T_{vd}$ at $t \simeq 0.5$ ($T_{vg} = T_r$, T_r, $T_{vd} = 0.15T_r$). (b) Simulation with function B and $T_{vg} < T_{vd}$ ($T_{vg} = 0.3\ T_r$,, $T_{vd} = 1.2T_r$). Also shown is simulation carried out with function C and $T_{vg} > T_{vd}$ ($T_{vg} = T_r$, $T_{vd} = 0.15\ T_r$) at (c) t = 0.15 and at (d) t = 0.4.

morphodynamics on the formation of vegetation patterns. River dynamics were expressed using a fluid-dynamic model able to reproduce realistic river evolution, while the riparian biomass distribution was modeled accounting for some of the main effects of river dynamics on riparian vegetation, i.e., groundwater table oscillations, disturbance due to floods, sedimentation.

[36] The numerical simulations highlight the emergence of well-defined vegetation patterns due to river movement. When the temporal scale of the vegetation is much lower than that of river dynamics, the riparian vegetation follows the river movements and always exhibits stationary density values with respect to the river axis. The most interesting patterns can be found when $T_v \simeq T_r$. In this case, the fundamental characteristic is the presence of an evident zone with low vegetation density in the internal part of the meander. This basic feature is independent of the biomass distribution along the river transect. However, several important details (e.g., the shape and extension of the low biomass zone, biomass gradients) are influenced by the different types of vegetation density profiles A, B, or C. The same aspects are also influenced by the timescales of the vegetation growth. The simulated vegetation patterns were also compared with some real cases, and good resemblances were found.

[37] Other factors, such as the presence of animals, fires, human actions, etc., can influence riparian vegetation evolution due to their disturbing action and these factors should not be ignored. However, all these actions, when they do not change river hydrology to a great extent (e.g., climate changes, construction of dams), usually modify the riparian vegetation patterns at a timescale which is

shorter than the morphodynamic one considered in our model. For this reason, these disturbances are not able to modify the general peculiarities of the patterns observed in the present simulations. Moreover, from our investigations of real cases, the influence of river migration on riparian vegetation seems to be widespread in nature and the fluvial processes seem to be the main factor that controls riparian vegetation evolution at the temporal scales have been investigated.

[38] Riparian vegetation-river dynamics constitute a very complex problem, with a great deal of linear and nonlinear interactions. Although certain modeling approximations were made during this work, the main purpose of the research was to start assessing the contribution of river migration to vegetation dynamics by means of a simple but realistic model, and stressing the necessity of coupling river morphodynamics to the vegetation evolution.

References

- Beck, S. (1984), Mathematical modelling of meander interaction, in *River Meandering,* edited by C. Elliott, pp. 932-941, Am. Soc. of Civ. Eng., New York.
- Bradley, C. E., and D. G. Smith (1986), Plains cottonwood recruitment and survival on a prairie meandering river floodplain, Milk River, southern Alberta and northern Montana, *Can. J. Bot., 64,* 1433-1442.
- Camporeale, C., P. Perona, A. Porporato, and L. Ridolfi (2005), On the long-term behavior of meandering rivers, *Water Resour. Res., 41,*W12403, doi:10.1029/2005WR004109.
- Carr, C. J. (1998), Patterns of vegetation along the Omo River in southwest Ethiopia, *Plant Ecol., 135,* 135-163.
- Carson, M., and M. Lapointe (1983), The inherent asymmetry of river meander planform, *J. Geol., 91,* 41 -55.
- Dietrich, W., and J. Smith (1983), Influence of point bar on flow through meander bends, *Water Resour. Res., 19,* 1173-1192.
- Howard, A. D. (1984), Simulation model of meandering, in *River Meandering,* edited by C. M. Elliott, pp. 952-963, Am. Soc. of Civ. Eng., New York.
- Hughes, F. (1997), Floodplain biogeomorphology, *Prog. Phys. Geogr., 21,*501 -529.
- Ikeda, S., and G. Parker (1989), *River Meandering, Water Resour. Monogr.,*vol. 12, AGU, Washington, D. C.
- Ikeda, S. G., G. Parker, and K. Sawai (1981), Bend theory of river meanders: 1. Linear development, *J. Fluid Mech., 112,* 363 -377.
- Johannesson, H., and G. Parker (1989), Linear theory of river meanders, in *River Meandering, Water Resour. Monogr.,* vol. 12, edited by S. Ikeda and G. Parker, pp. 181-214, AGU, Washington, D. C.
- Kinoshita, R. (1961), Investigation of channel deformation in Ishikari River, technical report, pp. 1 -174, Bureau of Resour., Dep. of Sci. and Technol., Tokyo.
- Mahoney, J., and S. Rood (1998), Stream flow requirements for cottonwood seedling recruitment—An integrative model, *Wetlands, 18,* 634-645.
- Malanson, G. (1993), *Riparian Landscapes,* Cambridge Univ. Press, NewYork.
- Mitsch, W., and J. Gosselink (2000), *Wetlands,* 3rd ed., John Wiley, Ho-boken, N. J.
- Naiman, R., and H. Decamps (1997), The ecology of interfaces: Riparian zones, *Annu. Rev. Ecol. Syst., 28,* 621 -658.
- Nanson, G. C., and H. F. Beach (1977), Forest succession and sedimentation on a meandering-river floodplain, North East British Columbia,Canada, *J. Biogeogr., 4,* 229-251.
- Parker, G., and H. Johannesson (1989), Observations on several recent theories of resonance and overdeepening in meandering channels, in *River Meandering, Water Resour. Monogr.,* vol. 12, pp. 379-415,AGU, Washington, D. C.
- Parker, G., P. Diplas, and J. Akiyama (1983), Meanders bends of high amplitude, *J. Hydraul. Eng.,* 109(10), 1323-1337.
- Pizzuto, J., and T. Meckelnburg (1989), Evaluation of a linear bank erosion equation, *Water Resour. Res., 25,* 1005-1013.
- Richter, B. D., and H. E. Richter (2000), Prescribing flood regimes to sustain riparian ecosystem along meandering rivers, *Conserv. Biol., 14,*1467-1478.

- Sun, T., T. Jossang, P. Meakin, and K. Schwarz (1996), Asimulation model for meandering rivers, *Water Resour. Res., 32,* 2937-2954.
- Thornley, J. H., and J. France (2005), An open-ended logistic-based growth function, *Ecol. Modell., 184,* 257-261.
- Tsoularis, A., and J. Wallace (2002), Analysis of logistic growth models, *Math. Biosci., 179,* 21 -55.
- Van De Wiel, M. J., and S. E. Darby (2004), Numerical modeling of bedtopography and bank erosion along tree-lined meandering rivers, in *Riparian Vegetation and Fluvial Geomorphology, Water Sci. Appl.,* vol. 8,